J. Fluid Mech. (1967), vol. 29, part 2, pp. 317–336
Printed in Great Britain

A non-linear theory for a full cavitating hydrofoil in a transverse gravity field

By BRUCE E. LAROCK† AND ROBERT L. STREET
Stanford University

(Received 6 September 1966)

An analysis is made of the effect of a transverse gravity field on a two-dimensional fully cavitating flow past a flat-plate hydrofoil. Under the assumption that the flow is both irrotational and incompressible, a non-linear method is developed by using conformal mapping and the solution to a mixed-boundary-value problem in an auxiliary half plane. A new cavity model, proposed by Tulin (1964*a*), is employed. The solution to the gravity-affected case was found by iteration; the non-gravity solution was used as the initial trial of a rapidly convergent process. The theory indicates that the lift and cavity size are reduced by the gravity field. Typical results are presented and compared to Parkin's (1957) linear theory.

1. Introduction

Few cavity-flow theories consider the influence of a gravity field. This neglect is usually justified on the ground that the effect of gravity is not large enough to counterbalance the mathematical complications encountered in trying to include it in the analysis. In addition, for high-speed operation (in excess of 40 knots) the effect of a gravity field on lift appears to be minor. Finally, many cavity flow solutions, as they are now formulated, cannot be extended to a proper consideration of the presence of gravity because of the attendant mathematical difficulties.

On the other hand, a small number of pertinent cavity-flow solutions which consider the effects of a gravity field do exist. All of these solutions contain mathematical simplifications or approximations, which are not needed in the following solution, or they treat a problem containing a physical symmetry which is not present in the current problem. Specifically, Parkin (1957) and Street (1963) presented linearized theories for flows in a transverse gravity field. They also use an additional approximation in their treatment of the boundary conditions in these problems. However, Street (1965) has shown this approximation to be quantitatively equivalent to a first-order solution in the smallness parameter $1/F^2$, and Kiceniuk & Acosta (1966) have verified the results experimentally. Acosta (1961) and Lenau & Street (1965) have presented linear and non-linear solutions, respectively, for a wedge symmetrically placed in a longitudinal gravity field; symmetry considerations allowed them to treat only one half of the flow field and hence to deal with only one free streamline in obtaining their solutions.

† Now at University of California (Davis).

In contrast to previous efforts, we present here an exact, non-linear solution to the unsymmetric problem of flow past a flat-plate hydrofoil, with finite trailing cavity, operating in a transverse gravity field and in an unbounded fluid. The solution is obtained via a rapidly convergent, direct iteration approach; this method, however, requires the use of a high-speed digital computer.

2. General theory

We consider a steady, two-dimensional, irrotational, and unbounded flow of an inviscid, incompressible, homogeneous fluid past a fully cavitating hydrofoil (see figure 1). For this flow the Bernoulli equation can be written as

$$p + \tfrac{1}{2}\rho q^2 + \rho g y = \text{constant}. \tag{2.1}$$

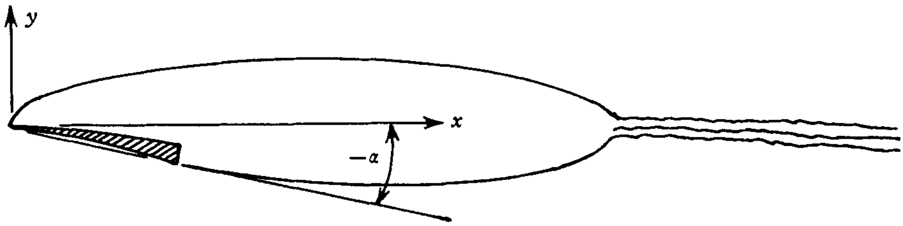

FIGURE 1. A fully cavitating hydrofoil.

In (2.1) p is the pressure, q is the magnitude of the fluid velocity, y is the vertical distance between a point in the fluid and some reference elevation, ρ is the fluid density, and g is the acceleration due to gravity. The constant above is the sum of the Bernoulli terms evaluated at the reference point at infinity where the flow is undisturbed. The reference elevation is chosen to be zero. Denoting reference quantities by a subscript 0, we obtain

$$p + \tfrac{1}{2}\rho q^2 + \rho g y = p_0 + \tfrac{1}{2}\rho q_0^2. \tag{2.2}$$

Two basic dimensionless quantities can be formed from the terms in (2.2), the cavitation number σ and the Froude number F,

$$\sigma = \frac{p_0 - p_c}{\frac{1}{2}\rho q_0^2}, \quad \text{and} \quad F^2 = \frac{q_0^2}{gl}, \tag{2.3}$$

where p_c is the constant pressure in the cavity and l is chosen to be the plate length. Note that when gravity is neglected $1/F^2$ is zero. If q_c is the fluid speed on the cavity free streamlines when $g = 0$, then from (2.2) and (2.3)

$$q_c = q_0(1+\sigma)^{\frac{1}{2}}. \tag{2.4}$$

On the cavity boundary the ratio of the fluid speed q in the presence of gravity to q_c can be expressed in terms of the cavitation and Froude numbers as

$$\frac{q}{q_c} = \left(1 - \frac{1}{1+\sigma}\frac{1}{F^2}\frac{2y}{l}\right)^{\frac{1}{2}}, \tag{2.5}$$

where q and y refer to the same point on the free streamline.

To model the physical flow, we employ the single-spiral-vortex model (Tulin 1964*a*); the analysis is based on the methods described by Larock & Street (1965). Figure 2 depicts the physical plane (z-plane) for a flat-plate hydrofoil using this model. The plate is inclined at an angle α in a parallel fluid flow, the undisturbed speed being q_0 at infinity. The co-ordinate origin is placed at the stagnation point with the x-axis parallel to the undisturbed flow. The flow separates smoothly from the ends of the plate. The characteristic or reference velocity is taken to be q_c; it is later normalized to unity.

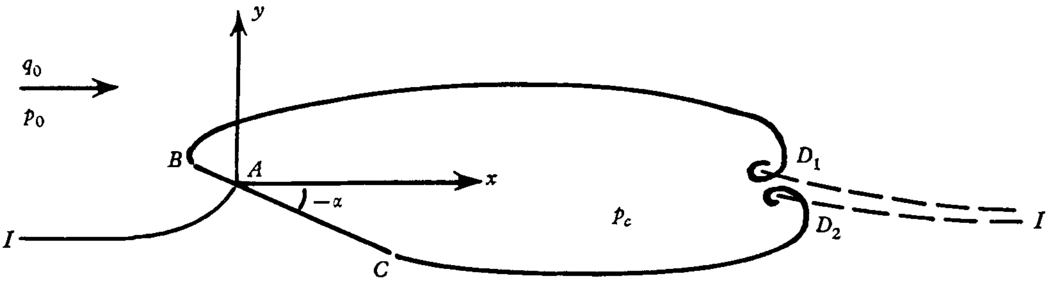

FIGURE 2. Single-spiral-vortex model.

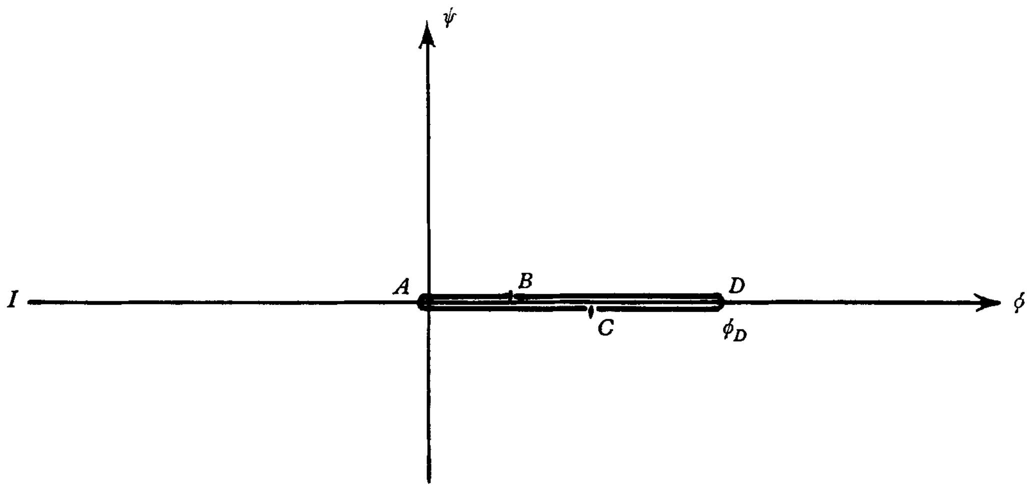

FIGURE 3. The W-plane for an infinite fluid.

For the assumed model and flow, the plane of the complex potential $W = \phi + i\psi$ is as shown in figure 3. The W-plane, the z-plane, and the normalized complex velocity ζ are related uniquely by

$$\zeta = \frac{1}{q_c}\frac{dW}{dz} = \frac{q}{q_c}e^{-i\theta}. \tag{2.6}$$

If (2.6) can be integrated, it will give the physical plane configuration as

$$z = \frac{1}{q_c}\int\frac{dW}{\zeta}. \tag{2.7}$$

The crux of the problem, then, is to determine W and ζ as functions of the same single variable so that (2.7) can be integrated. Toward this goal we determine W as a function of the half-plane variable t by conformal mapping. We then observe that either the direction or the magnitude of the complex velocity is known at each point along the flow boundaries. This information, used in conjunction with the Riemann–Hilbert technique, will enable us to construct ζ explicitly as a function of t. Once ζ is known, the fluid velocity itself is known, and the lift and drag coefficients of the foil can be determined by use of the Bernouilli equation. However, it is convenient to consider not ζ but the related function

$$\omega = \ln \zeta = \ln \frac{q}{q_c} + i(-\theta). \tag{2.8}$$

At a stagnation point (where $q = 0$), $\mathrm{Re}(\omega)$ now has a logarithmic singularity, and $\mathrm{Im}(\omega)$ has a jump discontinuity. The problem formulation will account for this behaviour.

The general solution of the Riemann–Hilbert mixed-boundary-value problem in an upper half plane is well known (Song 1963; Larock & Street 1965). If the imaginary part of some function $Q(t)$, $\mathrm{Im}[Q(t)]$, is known at all points on the boundary—i.e. on the real axis—then

$$Q(t) = \frac{1}{\pi}\int_{-\infty}^{\infty} \frac{\mathrm{Im}[Q(\tau)]}{\tau - t} d\tau + \Sigma A_j t^j \tag{2.9}$$

is a regular analytic function in the entire upper half plane. It remains to relate $\omega(t)$ to $Q(t)$ so that $\mathrm{Im}[Q(t)]$ is known at every point on the real line.

We map the W-plane to the t-plane so that the foil itself maps on to a finite segment of the t-plane boundary, and the cavity boundaries are mapped on to the remainder of the entire real line. Then, as we proceed from $-\infty$ to $+\infty$ on the real line, either $\mathrm{Re}(\omega)$ is known (on cavity boundaries) or $\mathrm{Im}(\omega)$ is known (on the foil).

Following Cheng & Rott (1954), we can convert these conditions to those of the Riemann–Hilbert problem itself. Hence, we must construct an auxiliary function $H(t)$, analytic for $\mathrm{Im}(t) > 0$, which, on the real axis, is purely imaginary where the real part of ω is known and is purely real where the imaginary part of ω is known. Then the imaginary part of the quotient $Q(t) = \omega(t)/H(t)$ is known on the entire real axis, as required.

A function satisfying the above requirements is

$$H(t) = -i[(t+1)(t-t_B)]^{\frac{1}{2}}, \tag{2.10}$$

where -1 and t_B correspond to the ends of the foil. We choose $\mathrm{Im}[H(t)] > 0$ on the real axis for $t < -1$ and select a branch cut on the real-axis interval $(-1, t_B)$ so that $H(t)$ is single-valued.

The combined use of the mapping and the Riemann–Hilbert technique introduces unknown constants into the problem. Two constants may be determined by requiring that the flow be uniform at infinity, since this condition places one constraint on each part of the complex velocity. In this unbounded flow it is also necessary to require the net source strength of the foil-cavity combination to be zero so that the cavity is closed. These conditions are sufficient to determine uniquely a set of physical and non-physical parameters which, upon insertion into the proper expressions, fully describe the physical flow.

Finally, it can be shown (Larock & Street 1965) that the lift L and drag D for the foil are related to the pressure difference across the foil by

$$D+iL = -i\int_l (p-p_c)\,dz, \tag{2.11}$$

where l denotes integration proceeding from tail to nose along the foil. Defining the lift and drag coefficients, respectively, as

$$C_L = \frac{L}{(\rho/2)q_c^2 l} \quad \text{and} \quad C_D = \frac{D}{(\rho/2)q_c^2 l}, \tag{2.12}$$

we can obtain an expression for (C_D+iC_L) as a function only of known quantities.

3. Analysis

We begin by mapping the W-plane on to the t-plane by choosing a three-point correspondence between planes to insure uniqueness of the mapping (Churchill 1960):

$$\left.\begin{array}{lll} A: & W=0 & t=0, \\ C: & W=e^{2\pi i} & t=-1, \\ D: & W=\phi_D & \operatorname{Re}|t|\to\infty. \end{array}\right\} \tag{3.1}$$

This choice of points maps the plate-cavity boundary D_2CABD_1 on to the real axis of the t-plane (figure 4). The mapping is

$$t = k\left[\frac{W}{\phi_D - W}\right]^{\frac{1}{2}}, \tag{3.2}$$

where

$$k^2 = \phi_D - 1. \tag{3.3}$$

The solution is based upon an iterative procedure which employs the non-gravity solution [then $g = 0$ in (2.1), (2.2), (2.3) and (2.5)] as the initial trial solution It is highly advantageous to use known properties of the nongravity solution in the formulation of the gravity solution, since in each case we use the same cavity model (the single-spiral-vortex model) and the same solution procedure [see Larock & Street (1965) for details].

We note immediately two items in our solution technique and model which provide distinct advantages over other approaches to the problem. First, we always know the location of the two free streamlines in the t-plane. Secondly, we know that, beyond some positive and negative value of t, $y(t)$ becomes essentially constant on each streamline because we are then in the tightly spiralling vortices that terminate the cavity. These two values of $y(t)$ are y_L and y_U for the lower and upper free streamlines, respectively; the t values where the constant y values initially apply are correspondingly t_L and t_U. Thus, for $t \leqslant t_L$, $y(t) = y_L$; for $t \geqslant t_U$, $y(t) = y_U$. The former item always permits the referencing of information about the free streamlines to known locations in the t-plane, independent of the effects of a gravity field. The latter item allows us to avoid numerical integration over the infinite intervals containing the free streamlines in the t-plane (see figure 4).

For this problem gravity acts parallel to the y-axis and in the negative direction; $y = 0$ is the reference elevation. According to (2.5), in the presence of gravity,

$$\left.\begin{aligned} \operatorname{Re}(\omega) &= \tfrac{1}{2}\ln\left[1-\frac{1}{1+\sigma}\frac{1}{F^2}\frac{2y(t)}{l}\right] && (-\infty < t < -1),\\ \operatorname{Im}(\omega) &= \alpha && (-1 < t < 0),\\ \operatorname{Im}(\omega) &= \alpha-\pi && (0 < t < t_B),\\ \operatorname{Re}(\omega) &= \tfrac{1}{2}\ln\left[1-\frac{1}{1+\sigma}\frac{1}{F^2}\frac{2y(t)}{l}\right] && (t_B < t < \infty). \end{aligned}\right\} \tag{3.4}$$

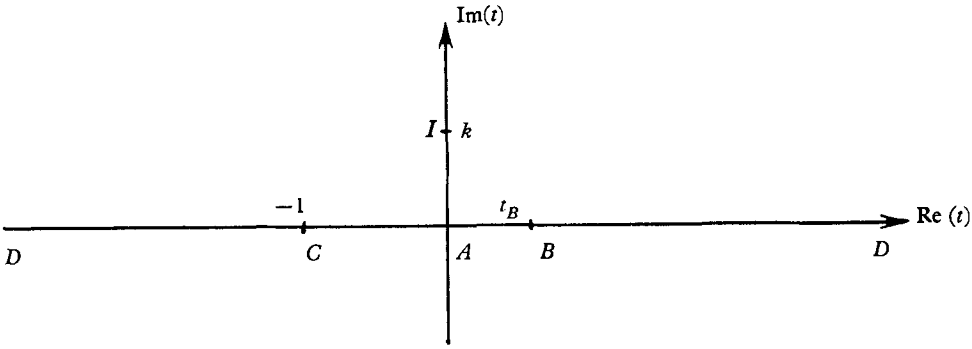

FIGURE 4. The t-plane for an infinite fluid.

We now form $\omega(t)/H(t)$ to obtain on $\operatorname{Im}(t) = 0$:

$$\left.\begin{aligned} \operatorname{Im}\left[\frac{\omega(t)}{H(t)}\right] &= -\tfrac{1}{2}\ln\left[1-\frac{1}{1+\sigma}\frac{1}{F^2}\frac{2y(t)}{l}\right][(1+t)(t-t_B)]^{-\frac{1}{2}} && (-\infty < t < -1),\\ \operatorname{Im}\left[\frac{\omega(t)}{H(t)}\right] &= \alpha[(t_B-t)(1+t)]^{-\frac{1}{2}} && (-1 < t < 0),\\ \operatorname{Im}\left[\frac{\omega(t)}{H(t)}\right] &= (\alpha-\pi)[(t_B-t)(1+t)]^{-\frac{1}{2}} && (0 < t < t_B),\\ \operatorname{Im}\left[\frac{\omega(t)}{H(t)}\right] &= \tfrac{1}{2}\ln\left[1-\frac{1}{1+\sigma}\frac{1}{F^2}\frac{2y(t)}{l}\right][(1+t)(t-t_B)]^{-\frac{1}{2}} && (t_B < t < \infty). \end{aligned}\right\} \tag{3.5}$$

It can be shown (Larock & Street 1965) that $\omega \sim t$ on the real axis as $|t| \to \infty$. Noting that $|H(t)| \sim t$ on the axis as $|t| \to \infty$, we conclude that $\omega(t)/H(t)$ must asymptotically become a constant. Limitations on allowable singularity strength exclude negative powers of t in the series of (2.9). Therefore, the series can have at most one non-zero term corresponding to $j = 0$ (we let $A_0 = A$).

The mathematical representation for ω is now

$$\omega(t) = H(t)\left\{-\frac{1}{2\pi}\int_{-\infty}^{-1}\frac{\ln\left[1-\frac{1}{1+\sigma}\frac{1}{F^2}\frac{2y(\eta)}{l}\right]d\eta}{(\eta-t)[(1+\eta)(\eta-t_B)]^{\frac{1}{2}}}\right.$$

$$+\frac{\alpha}{\pi}\int_{-1}^{t_B}\frac{d\eta}{(\eta-t)[(1+\eta)(t_B-\eta)]^{\frac{1}{2}}}-\int_{0}^{t_B}\frac{d\eta}{(\eta-t)[(1+\eta)(t_B-\eta)]^{\frac{1}{2}}}$$

$$\left.+\frac{1}{2\pi}\int_{t_B}^{\infty}\frac{\ln\left[1-\frac{1}{1+\sigma}\frac{1}{F^2}\frac{2y(\eta)}{l}\right]d\eta}{(\eta-t)[(1+\eta)(\eta-t_B)]^{\frac{1}{2}}}+A\right\}. \tag{3.6}$$

When we apply the conditions that the flow at infinity be undisturbed and that the cavity close, we obtain three independent equations in the unknown parameters k, t_B and A.

At infinity, which corresponds to $t = ik$, we have $q = q_0$ and $\theta = 0$, so

$$\mathrm{Re}\,[\omega(ik)] = \ln\frac{q_0}{q_c} = -\tfrac{1}{2}\ln(1+\sigma) \tag{3.7}$$

and

$$\mathrm{Im}\,[\omega(ik)] = 0. \tag{3.8}$$

Parkin (1959) indicates that the net flux of fluid out of any closed contour C is proportional to $\mathrm{Im}\oint_C \zeta(z)\,dz$. Expressing ζ as a power series in descending powers of z for large z reveals that the singularities of ω are the same as those of ζ. Hence, for zero net source strength, we have, with C enclosing the body-cavity system,

$$\mathrm{Im}\oint_C \zeta\,dz = \mathrm{Im}\oint_C \omega\,dz = \mathrm{Im}\oint_C \omega\,dW = 0,$$

using the fact that a source remains a source under conformal transformation (Milne-Thompson 1960). This result then becomes

$$\mathrm{Im}\oint_C \omega(t)\frac{dW}{dt}\,dt = 0, \tag{3.9}$$

with C now enclosing the upper half plane. We calculate

$$\frac{dW}{dt} = \frac{2k^2(k^2+1)t}{(t+ik)^2(t-ik)^2} = \frac{2k^2(k^2+1)t}{(t^2+k^2)^2}, \tag{3.10}$$

which is singular only at $t = ik$ and asymptotically is $O(t^{-3})$ so that the integrand $\omega(dW/dt)$ is non-singular as $|t|\to\infty$. Near the stagnation point on the plate, the integrand—as can be verified from (4.1) below—is $O(t\ln t)\to 0$ as $t\to 0$ and so is non-singular. Therefore, we obtain our third condition by applying the calculus of residues to (3.9). Thus,

$$\mathrm{Im}\left[\frac{d\omega(t)}{dt}\right]_{t=ik} = 0, \tag{3.11}$$

or

$$\operatorname{Im}[\omega'(ik)] = \operatorname{Im}\left[\frac{H'(ik)}{H(ik)}\omega(ik) + H(ik)\left\{-\frac{1}{2\pi}\int_{-\infty}^{-1}\frac{\ln\left[1-\frac{1}{1+\sigma}\frac{1}{F^2}\frac{2y(\eta)}{l}\right]d\eta}{(\eta-ik)^2[(1+\eta)(\eta-t_B)]^{\frac{1}{2}}}\right.\right.$$
$$+\frac{\alpha}{\pi}\int_{-1}^{t_B}\frac{d\eta}{(\eta-ik)^2[(1+\eta)(t_B-\eta)]^{\frac{1}{2}}} - \int_0^{t_B}\frac{d\eta}{(\eta-ik)^2[(1+\eta)(t_B-\eta)]^{\frac{1}{2}}}$$
$$\left.\left.+\frac{1}{2\pi}\int_{t_B}^{\infty}\frac{\ln\left[1-\frac{1}{1+\sigma}\frac{1}{F^2}\frac{2y(\eta)}{l}\right]d\eta}{(\eta-ik)^2[(1+\eta)(\eta-t_B)]^{\frac{1}{2}}}\right\}\right] = 0. \tag{3.12}$$

The integrals in (3.12) are expressible in terms of the integrals occurring in $\omega(ik)$ (see Larock & Street 1966).

From above, we have

$$\omega(ik) = -i[(ik+1)(ik-t_B)]^{\frac{1}{2}}\left\{-\frac{1}{2\pi}\int_{-\infty}^{-1}\frac{\ln\left[1-\frac{1}{1+\sigma}\frac{1}{F^2}\frac{2y(\eta)}{l}\right]d\eta}{(\eta-ik)[(1+\eta)(\eta-t_B)]^{\frac{1}{2}}}\right.$$
$$+\frac{\alpha}{\pi}\int_{-1}^{t_B}\frac{d\eta}{(\eta-ik)[(1+\eta)(t_B-\eta)]^{\frac{1}{2}}} - \int_0^{t_B}\frac{d\eta}{(\eta-ik)[(1+\eta)(t_B-\eta)]^{\frac{1}{2}}}$$
$$\left.+\frac{1}{2\pi}\int_{t_B}^{\infty}\frac{\ln\left[1-\frac{1}{1+\sigma}\frac{1}{F^2}\frac{2y(\eta)}{l}\right]d\eta}{(\eta-ik)[(1+\eta)(\eta-t_B)]^{\frac{1}{2}}}+A\right\}. \tag{3.13}$$

These integrals are more easily evaluated first in complex form (see Larock & Street 1966) and then split into their real and imaginary parts. Further algebraic manipulation will then yield the final equations resulting from the application of the boundary condition equations (3.7), (3.8) and (3.12).

The three equations ultimately resulting from the boundary conditions are

$$\tfrac{1}{2}\ln(1+\sigma) - A\beta_1 = \beta_1 I_1 - \beta_2 I_2 - \frac{\beta_1}{2\pi}[I_5(t_L,-1) - I_5(t_B,t_U)] + \frac{k\beta_2}{2\pi}[I_6(t_L,-1)$$
$$-I_6(t_B,t_U)] + \frac{1}{2\pi}\left\{E_1\ln\left[1-\frac{1}{1+\sigma}\frac{1}{F^2}\frac{2y_L}{l}\right] + E_2\ln\left[1-\frac{1}{1+\sigma}\frac{1}{F^2}\frac{2y_U}{l}\right]\right\}, \tag{3.14}$$

$$\alpha - A\beta_2 = \beta_1 I_2 + \beta_2 I_1 - \frac{\beta_2}{2\pi}[I_5(t_L,-1) - I_5(t_B,t_U)] - \frac{k\beta_1}{2\pi}[I_6(t_L,-1) - I_6(t_B,t_U)]$$
$$-\frac{1}{4\pi}\left\{E_3\ln\left[1-\frac{1}{1+\sigma}\frac{1}{F^2}\frac{2y_L}{l}\right] + E_4\ln\left[1-\frac{1}{1+\sigma}\frac{1}{F^2}\frac{2y_U}{l}\right]\right\}, \tag{3.15}$$

and

$$-\frac{k}{4}\left(\frac{1}{k^2+1}+\frac{1}{k^2+t_B^2}\right)\ln(1+\sigma) + \frac{1}{2}\frac{\alpha(k^2-t_B)(1-t_B)}{(k^2+t_B)^2+(1-t_B)^2k^2}$$
$$= \frac{\beta_1 t_B^{\frac{1}{2}}}{k[(k^2+t_B)^2+(1-t_B)^2k^2]^{\frac{1}{2}}} + \frac{1}{(k^2+t_B)^2+(1-t_B)^2k^2}$$
$$\times\{\tfrac{1}{2}(k^2-t_B)(1-t_B)(\beta_1 I_2+\beta_2 I_1) - k[k^2+\tfrac{1}{2}(1+t_B^2)](\beta_1 I_1 - \beta_2 I_2)\}$$

$$+\frac{\beta_2}{2\pi}[I_7(t_L,-1)-I_7(t_B,t_U)]+\frac{k\beta_1}{\pi}[I_8(t_L,-1)-I_8(t_B,t_U)]$$

$$+\frac{1}{2\pi}\ln\left(1-\frac{1}{1+\sigma}\frac{1}{F^2}\frac{2y_L}{l}\right)\left[\frac{1}{(k^2+t_B)^2+(1-t_B)^2k^2}\{(k^2+t_B)[-\tfrac{1}{4}(1-t_B)E_3+kE_1]\right.$$

$$\left.+\tfrac{1}{2}k(1-t_B)[kE_3+(1-t_B)E_1]\}+\frac{k\beta_1-t_L\beta_2}{(\beta_1^2+\beta_2^2)(t_L^2+k^2)}[(1+t_L)(t_L-t_B)]^{\frac{1}{2}}-\frac{\beta_2}{\beta_1^2+\beta_2^2}\right]$$

$$-\frac{1}{2\pi}\ln\left(1-\frac{1}{1+\sigma}\frac{1}{F^2}\frac{2y_U}{l}\right)\left[\frac{1}{(k^2+t_B)^2+(1-t_B)^2k^2}\{(k^2+t_B)[\tfrac{1}{4}(1-t_B)E_4-kE_2]\right.$$

$$\left.-\tfrac{1}{2}k(1-t_B)[kE_4+(1-t_B)E_2]\}+\frac{\beta_2t_U-\beta_1k}{(\beta_1^2+\beta_2^2)(t_U^2+k^2)}[(1+t_U)(t_U-t_B)]^{\frac{1}{2}}-\frac{\beta_2}{\beta_1^2+\beta_2^2}\right].\tag{3.16}$$

In these equations

$$\delta^2=[(k^2+t_B)^2+k^2(1-t_B)^2]^{\frac{1}{2}},\tag{3.17a}$$

$$\beta_1=-[\tfrac{1}{2}(k^2+t_B)+\tfrac{1}{2}\delta^2]^{\frac{1}{2}},\qquad \beta_2=[-\tfrac{1}{2}(k^2+t_B)+\tfrac{1}{2}\delta^2]^{\frac{1}{2}},\tag{3.17b}$$

$$\left.\begin{aligned}\beta_3&=-[-\tfrac{1}{2}+\tfrac{1}{2}(1+k^2)^{\frac{1}{2}}]^{\frac{1}{2}},\qquad \beta_4=[\tfrac{1}{2}+\tfrac{1}{2}(1+k^2)^{\frac{1}{2}}]^{\frac{1}{2}},\\ \beta_5&=[-\tfrac{1}{2}t_B+\tfrac{1}{2}(t_B+k^2)^{\frac{1}{2}}]^{\frac{1}{2}},\qquad \beta_6=[\tfrac{1}{2}t_B+\tfrac{1}{2}(t_B+k^2)^{\frac{1}{2}}]^{\frac{1}{2}},\end{aligned}\right\}\tag{3.17c}$$

and

$$I_5(\eta_1,\eta_2)=\int_{\eta_1}^{\eta_2}\frac{\eta\ln\left[1-\dfrac{1}{1+\sigma}\dfrac{1}{F^2}\dfrac{2y(\eta)}{l}\right]d\eta}{(\eta^2+k^2)[(1+\eta)(\eta-t_B)]^{\frac{1}{2}}},\tag{3.17d}$$

$$I_6(\eta_1,\eta_2)=\int_{\eta_1}^{\eta_2}\frac{\ln\left[1-\dfrac{1}{1+\sigma}\dfrac{1}{F^2}\dfrac{2y(\eta)}{l}\right]d\eta}{(\eta^2+k^2)[(1+\eta)(\eta-t_B)]^{\frac{1}{2}}},\tag{3.17e}$$

$$I_7(\eta_1,\eta_2)=\int_{\eta_1}^{\eta_2}\frac{(\eta^2-k^2)\ln\left[1-\dfrac{1}{1+\sigma}\dfrac{1}{F^2}\dfrac{2y(\eta)}{l}\right]d\eta}{(\eta^2+k^2)^2[(1+\eta)(\eta-t_B)]^{\frac{1}{2}}},\tag{3.17f}$$

$$I_8(\eta_1,\eta_2)=\int_{\eta_1}^{\eta_2}\frac{\eta\ln\left[1-\dfrac{1}{1+\sigma}\dfrac{1}{F^2}\dfrac{2y(\eta)}{l}\right]d\eta}{(\eta^2+k^2)^2[(1+\eta)(\eta-t_B)]^{\frac{1}{2}}},\tag{3.17g}$$

while

$$\left.\begin{aligned}P_1&=\beta_5+\beta_3t_B^{\frac{1}{2}},\quad P_2=\beta_5-\beta_3t_B^{\frac{1}{2}},\\ Q_1&=\beta_6+\beta_4t_B^{\frac{1}{2}},\quad Q_2=\beta_6-\beta_4t_B^{\frac{1}{2}},\end{aligned}\right\}\tag{3.17h}$$

$$\Omega(\eta_1,\eta_2)=\begin{cases}0 & \eta_1=\eta_2=0,\\ \tan^{-1}(\eta_2/\eta_1) & \eta_1>0,\quad \text{all } \eta_2,\\ \tfrac{1}{2}\pi & \eta_1=0,\quad \eta_2>0,\\ -\tfrac{1}{2}\pi & \eta_1=0,\quad \eta_2<0,\\ \pi+\tan^{-1}(\eta_2/\eta_1) & \eta_1<0,\quad \eta_2\geqslant 0,\\ -\pi+\tan^{-1}(\eta_2/\eta_1) & \eta_1<0,\quad \eta_2<0,\end{cases}\tag{3.17i}$$

$$\left.\begin{aligned} P_3 &= -2\beta_2+1-t_B, & Q_3 &= 2(k+\beta_1),\\ P_4 &= 2\beta_2+1-t_B, & Q_4 &= 2(k-\beta_1),\end{aligned}\right\} \tag{3.17j}$$

$$\left.\begin{aligned} P_5(\eta) &= 1-t_B+\left(\frac{2}{\eta^2+k^2}\right)\{(\eta\beta_2+k\beta_1)[(1+\eta)(\eta-t_B)]^{\frac{1}{2}}-\eta(k^2+t_B)-k^2(1-t_B)\},\\ Q_5(\eta) &= 2k+\left(\frac{2}{\eta^2+k^2}\right)\{(k\beta_2-\eta\beta_1)[(1+\eta)(\eta-t_B)]^{\frac{1}{2}}-k(k^2+t_B)+\eta k(1-t_B)\},\end{aligned}\right\} \tag{3.17k}$$

$$\left.\begin{aligned} E_1 &= \Omega(P_5(t_L),Q_5(t_L))-\Omega(P_3,Q_3), & E_2 &= \Omega(P_5(t_U),Q_5(t_U))-\Omega(P_4,Q_4),\\ E_3 &= \ln\left[\frac{P_5^2(t_L)+Q_5^2(t_L)}{P_3^2+Q_3^2}\right], & E_4 &= \ln\left[\frac{P_5^2(t_U)+Q_5^2(t_U)}{P_4^2+Q_4^2}\right],\end{aligned}\right\} \tag{3.17l}$$

$$I_1 = \frac{\beta_1}{2\delta^2}[\ln(P_1^2+Q_1^2)-\ln(P_2^2+Q_2^2)]+\frac{\beta_2}{\delta^2}\left[\Theta-\tan^{-1}\left(\frac{Q_2}{P_2}\right)\right], \tag{3.17m}$$

$$I_2 = \frac{\beta_2}{2\delta^2}[\ln(P_2^2+Q_2^2)-\ln(P_1^2+Q_1^2)]+\frac{\beta_1}{\delta^2}\left[\Theta-\tan^{-1}\left(\frac{Q_2}{P_2}\right)\right], \tag{3.17n}$$

with

$$\Theta = \begin{cases} \tan^{-1}\left(\dfrac{Q_1}{P_1}\right) & \text{if } P_1 > 0,\\ \frac{1}{2}\pi & \text{if } P_1 = 0,\\ \pi+\tan^{-1}\left(\dfrac{Q_1}{P_1}\right) & \text{if } P_1 < 0.\end{cases} \tag{3.17o}$$

Assuming the right sides of (3.14), (3.15) and (3.16) to be known, we can solve them for $\ln(1+\sigma)$, α and A from given values of k, t_B and F^2. For the right sides to be known, however, the free-streamline ordinates $y(t)$ must be known or approximated in some way. The same is true for σ and l, which also appear on the right side of the equations. In what follows we assume that σ, α and A are known quantities satisfying (3.14), (3.15) and (3.16).

4. Results

Results include the lift and drag coefficients and the plate-cavity configuration. We normalize on the non-gravity free-streamline speed so that $q_c = 1$ in the expressions which follow.

On the plate we obtain, upon integration of (3.6) for $-1 \leqslant t \leqslant t_B$,

$$\begin{aligned} \omega(t) = {} & i\alpha+\ln\left\{\frac{[t_B-t]^{\frac{1}{2}}-[t_B(1+t)]^{\frac{1}{2}}}{[t_B-t]^{\frac{1}{2}}+[t_B(1+t)]^{\frac{1}{2}}}\right\}+A[(t_B-t)(1+t)]^{\frac{1}{2}}+J_l(t)\\ & +\frac{1}{2\pi}\ln\left[1-\frac{1}{1+\sigma}\frac{1}{F^2}\frac{2y_L}{l}\right]\left\{\sin^{-1}\left[\frac{2\left[\dfrac{(1+t)(t-t_B)}{t_L-t}\right]+(1-t_B+2t)}{1+t_B}\right]\right.\\ & \left.-\sin^{-1}\left[\frac{1-t_B+2t}{1+t_B}\right]\right\}+\frac{1}{2\pi}\ln\left[1-\frac{1}{1+\sigma}\frac{1}{F^2}\frac{2y_U}{l}\right]\\ & \times\left\{\sin^{-1}\left[\frac{2\left[\dfrac{(1+t)(t_B-t)}{t_U-t}\right]-(1-t_B+2t)}{1+t_B}\right]-\sin^{-1}\left[\frac{-(1-t_B+2t)}{1+t_B}\right]\right\},\end{aligned} \tag{4.1}$$

where

$$J_l(t) = \frac{1}{2\pi}[(1+t)(t_B-t)]^{\frac{1}{2}}\left\{\int_{t_B}^{t_U}\frac{\ln\left[1-\frac{1}{1+\sigma}\frac{1}{F^2}\frac{2y(\eta)}{l}\right]d\eta}{(\eta-t)[(1+\eta)(\eta-t_B)]^{\frac{1}{2}}} - \int_{t_L}^{-1}\frac{\ln\left[1-\frac{1}{1+\sigma}\frac{1}{F^2}\frac{2y(\eta)}{l}\right]d\eta}{(\eta-t)[(1+\eta)(\eta-t_B)]^{\frac{1}{2}}}\right\} \quad (4.2)$$

is a continuous function of t. It can be shown that

$$\left.\begin{aligned} J_l(t_B) &= \tfrac{1}{2}\ln\left[1-\frac{1}{1+\sigma}\frac{1}{F^2}\frac{2y_B}{l}\right], \\ \text{and}\qquad J_l(-1) &= \tfrac{1}{2}\ln\left[1-\frac{1}{1+\sigma}\frac{1}{F^2}\frac{2y_C}{l}\right]. \end{aligned}\right\} \quad (4.3)$$

A numerical investigation indicated that the last two terms of (4.1) (each beginning with the factor $\frac{1}{2}\pi$) are usually extremely small and have no influence upon the results. These two terms will be deleted from the final expressions for the plate length and the force coefficients, but the addition of these terms to the expressions is straightforward. Applying (2.7) and (2.8) then gives the plate length

$$l = I_p(-1, t_B), \quad (4.4)$$

with

$$I_p(\eta_1,\eta_2) = \frac{4k^2(k^2+1)}{1+t_B}\int_{\eta_1}^{\eta_2}\left\{t_B-\left(\frac{1-t_B}{2}\right)t+[t_B(t_B-t)(1+t)]^{\frac{1}{2}}\right\} \times \exp\{-A[(1+t)(t_B-t)]^{\frac{1}{2}}-J_l(t)\}\frac{dt}{(k^2+t^2)^2}. \quad (4.5)$$

The end-point co-ordinates of the plate are

$$z_B = x_B+iy_B = (-\cos\alpha+i\sin\alpha)I_p(0,t_B), \quad (4.6)$$

$$z_C = x_C+iy_C = (+\cos\alpha-i\sin\alpha)I_p(-1,0). \quad (4.7)$$

Expressions for the lift and drag coefficients are derived next. From the Bernoulli equation (2.2),

$$\frac{p-p_c}{(\rho/2)q_c^2} = 1-\left(\frac{q}{q_c}\right)^2-\frac{1}{1+\sigma}\frac{1}{F^2}\frac{2y}{l}. \quad (4.8)$$

Using (2.11) and (2.12) gives

$$\begin{aligned} C_D+iC_L &= -i\left(\frac{1}{l}\right)\int_l\left[1-\left(\frac{q}{q_c}\right)^2-\frac{1}{1+\sigma}\frac{1}{F^2}\frac{2y}{l}\right]dz \\ &= -i\left(\frac{1}{l}\right)\left\{\int_{z_C}^{z_B}\left[1-\frac{1}{1+\sigma}\frac{1}{F^2}\frac{2y}{l}\right]dz-\int_{-1}^{t_B}\bar{\zeta}\frac{dW}{dt}dt\right\}, \end{aligned} \quad (4.9)$$

or

$$C_D = (1+I_c)\sin\alpha+\frac{1}{1+\sigma}\frac{1}{F^2}\frac{1}{l^2}(y_C^2-y_B^2) \quad (4.10)$$

and

$$C_L = (1+I_c)\cos\alpha+\frac{1}{1+\sigma}\frac{1}{F^2}\frac{1}{l^2}(x_C^2-x_B^2)\tan\alpha, \quad (4.11)$$

where
$$I_c = \frac{4k^2(k^2+1)}{l(1+t_B)} \int_{-1}^{t_B} \left\{ -t_B + \left(\frac{1-t_B}{2}\right) t + [t_B(t_B-t)(1+t)]^{\frac{1}{2}} \right\} \times \exp\{A[(t_B-t)(1+t)]^{\frac{1}{2}} + J_l(t)\} \frac{dt}{(k^2+t^2)^2}. \tag{4.12}$$

We next determine $\omega(t)$ on the streamlines as

$$\omega(t) = i\alpha + \tfrac{1}{2}\ln\left[1 - \frac{1}{1+\sigma}\frac{1}{F^2}\frac{2y(t)}{l}\right] - \ln\left\{\frac{-2t_B + t(1-t_B) \pm 2i[t_B(1+t)(t-t_B)]^{\frac{1}{2}}}{t(1+t_B)}\right\}$$
$$- iAt\left[\left(1+\frac{1}{t}\right)\left(1-\frac{t_B}{t}\right)\right]^{\frac{1}{2}} - iJ(t) \pm \left\{ -\ln\left[1 - \frac{1}{1+\sigma}\frac{1}{F^2}\frac{2y_L}{l}\right]\right.$$
$$\times \ln\left[\frac{\frac{2}{(t_L-t)}[(1+t)(t-t_B)(1+t_L)(t_L-t_B)]^{\frac{1}{2}} + \left(\frac{2}{t_L-t}\right)(1+t)(t-t_B) + 1 - t_B + 2t}{-2[(1+t)(t-t_B)]^{\frac{1}{2}} + 1 - t_B + 2t}\right]$$
$$- \ln\left[1 - \frac{1}{1+\sigma}\frac{1}{F^2}\frac{2y_U}{l}\right]$$
$$\left.\times \ln\left[\frac{\left(\frac{2}{t_U-t}\right)[(1+t)(t-t_B)(1+t_U)(t_U-t_B)]^{\frac{1}{2}} + \left(\frac{2}{t_U-t}\right)(1+t)(t-t_B) + 1 - t_B + 2t}{2[(1+t)(t-t_B)]^{\frac{1}{2}} + 1 - t_B + 2t}\right]\right\}, \tag{4.13}$$

where the $(+)$ signs apply for $t \geqslant t_B$, and the $(-)$ signs are used for $t < -1$. The function $J(t)$ is defined to be

$$J(t) = \frac{1}{2\pi} t\left[\left(1+\frac{1}{t}\right)\left(1-\frac{t_B}{t}\right)\right]^{\frac{1}{2}} \left\{ \int_{t_B}^{t-\epsilon} \frac{\ln\left[1 - \frac{1}{1+\sigma}\frac{1}{F^2}\frac{2y(\eta)}{l}\right] d\eta}{(\eta-t)[(1+\eta)(\eta-t_B)]^{\frac{1}{2}}} \right.$$
$$\left. + \int_{t+\epsilon}^{t_U} \frac{\ln\left[1 - \frac{1}{1+\sigma}\frac{1}{F^2}\frac{2y(\eta)}{l}\right] d\eta}{(\eta-t)[(1+\eta)(\eta-t_B)]^{\frac{1}{2}}} - \int_{t_L}^{-1} \frac{\ln\left[1 - \frac{1}{1+\sigma}\frac{1}{F^2}\frac{2y(\eta)}{l}\right] d\eta}{(\eta-t)[(1+\eta)(\eta-t_B)]^{\frac{1}{2}}} \right\} \tag{4.14}$$

for $t > t_B$, and

$$J(t) = \frac{1}{2\pi} t\left[\left(1+\frac{1}{t}\right)\left(1-\frac{t_B}{t}\right)\right]^{\frac{1}{2}} \left\{ \int_{t_B}^{t_U} \frac{\ln\left[1 - \frac{1}{1+\sigma}\frac{1}{F^2}\frac{2y(\eta)}{l}\right] d\eta}{(\eta-t)[(1+\eta)(\eta-t_B)]^{\frac{1}{2}}} \right.$$
$$\left. - \int_{t_L}^{t-\epsilon} \frac{\ln\left[1 - \frac{1}{1+\sigma}\frac{1}{F^2}\frac{2y(\eta)}{l}\right] d\eta}{(\eta-t)[(1+\eta)(\eta-t_B)]^{\frac{1}{2}}} - \int_{t+\epsilon}^{-1} \frac{\ln\left[1 - \frac{1}{1+\sigma}\frac{1}{F^2}\frac{2y(\eta)}{l}\right] d\eta}{(\eta-t)[(1+\eta)(\eta-t_B)]^{\frac{1}{2}}} \right\} \tag{4.15}$$

for $t < -1$. Further investigation shows that $J(t_B) = J(-1) = 0$. Upon substitution into (2.7), we find that the parametric representation for the streamlines which form the cavity boundary are

$$x - x_0 = \frac{4k^2(k^2+1)}{1+t_B} \int_{t_0}^{t} \left\{ \left(\frac{1-t_B}{2} - \frac{t_B}{t}\right) \cos[B(t) - \alpha] \right.$$
$$\left. - \left[t_B\left(1+\frac{1}{t}\right)\left(1-\frac{t_B}{t}\right)\right]^{\frac{1}{2}} \sin[B(t)-\alpha] \right\} \frac{t\,dt}{\left[1 - \frac{1}{1+\sigma}\frac{1}{F^2}\frac{2y(t)}{l}\right]^{\frac{1}{2}} (k^2+t^2)^2} \tag{4.16}$$

and

$$y-y_0 = \frac{4k^2(k^2+1)}{1+t_B}\int_{t_0}^{t}\left\{\left(\frac{1-t_B}{2}-\frac{t_B}{t}\right)\sin\left[B(t)-\alpha\right] + \left[t_B\left(1+\frac{1}{t}\right)\left(1-\frac{t_B}{t}\right)\right]^{\frac{1}{2}}\cos\left[B(t)-\alpha\right]\right\}\frac{t\,dt}{\left[1-\frac{1}{1+\sigma}\frac{1}{F^2}\frac{2y(t)}{l}\right]^{\frac{1}{2}}(k^2+t^2)^2}, \quad (4.17)$$

where

$$B(t) = At\left[\left(1+\frac{1}{t}\right)\left(1-\frac{t_B}{t}\right)\right]^{\frac{1}{2}} + J(t) \pm \left\{\ln\left[1-\frac{1}{1+\sigma}\frac{1}{F^2}\frac{2y_L}{l}\right] \times \ln\left[\frac{\left(\frac{2}{t_L-t}\right)[(1+t)(t-t_B)(1+t_L)(t_L-t_B)]^{\frac{1}{2}} + \left(\frac{2}{t_L-t}\right)(1+t)(t-t_B)+1-t_B+2t}{-2[(1+t)(t-t_B)]^{\frac{1}{2}}+1-t_B+2t}\right] + \ln\left[1-\frac{1}{1+\sigma}\frac{1}{F^2}\frac{2y_U}{l}\right] \times \ln\left[\frac{\left(\frac{2}{t_U-t}\right)[(1+t)(t-t_B)(1+t_U)(t_U-t_B)]^{\frac{1}{2}} + \left(\frac{2}{t_U-t}\right)(1+t)(t-t_B)+1-t_B+2t}{2[(1+t)(t-t_B)]^{\frac{1}{2}}+1-t_B+2t}\right]\right\}. \quad (4.18)$$

For the upper streamline $x_0 = x_B$, $y_0 = y_B$, $t_0 = t_B$, $t > t_B$, and the $(+)$ sign is used in $B(t)$. For the lower streamline $x_0 = x_C$, $y_0 = y_C$, $t_0 = -1$, $t < -1$, and the $(-)$ sign is used in $B(t)$.

5. The solution procedure

We consider the nature of solutions to the Laplace equation, our governing partial differential equation. The Laplace equation is elliptic; physically, this means that the boundary value data at each point on the boundary of our flow will affect the solution at every other point in the flow and, in particular, along the rest of the boundary. Equation (4.17) illustrates this property quite clearly.

Equation (4.17) purports to give an expression for $y(t)$, which is found on the left side of the equation. But $y(t)$ appears in the denominator of the integrand, and the integral of a function containing $y(t)$ appears in $J(t)$, which in turn appears in $B(t)$, a factor in the integrand. In addition, α, σ, A and l were determinable only because $y(t)$ was assumed to be known. In fact, the equations of §§3 and 4 may be thought of as a set of integral equations which define $y(t)$. These equations are of such complexity that most formal methods of integral equation theory are not useful. However, some integral equations are commonly solved by successive approximation, and proofs of uniform convergence and uniqueness of the solution are available for certain simple cases (Mikhlin 1964).

On the other hand, most analyses neglect gravity effects on the ground that they are relatively small (we postulate that they are not negligible, however). If this premise is true, then the non-gravity solution of Larock & Street (1965) should be a good approximation in some sense to an associated flow which is affected by gravity. In so far as the term

$$\left(\frac{1}{1+\sigma}\frac{1}{F^2}\frac{2y}{l}\right)$$

is small compared to unity, we are assured by the continuity of the Laplace equation (small changes in boundary data produce small changes in the solution [Weinberger 1965, p. 6]) that the preceding is true. Then, if the problem has been properly formulated, it should be possible successively to improve upon the initial approximation until, after a sufficient number of 'improvements', the correct solution to the gravity problem is indeed found. In our iteration method the complete solution is computed in each cycle. This procedure is in contrast to the perturbation method of solution in which the initial problem is expanded into a series of problems, each representing a different magnitude of approximation in an asymptotic solution. In the perturbation method, accuracy is improved only by the successive, complete, and exact solution of the next higher order-of-magnitude problem.

The iteration procedure for the present problem works in the following manner.

1. A suitable choice for k and t_B is made; more will be said later (see §6) on what constitutes a suitable choice.

2. The non-gravity solution ($g = 0$) is completed for this k and t_B; the parameters and the physical plane (especially $y(t)$ on the streamlines) are determined. We note that when $g = 0$ all results can be obtained without prior knowledge of $y(t)$.

3. New α, σ and A are then computed from (3.14), (3.15) and (3.16), using data from step 2 where appropriate. The function $J_l(t)$ is determined next, and l is computed [cf. (4.2) to (4.5)]. Then the gravity solution is completed, using $y(t)$ from step 2 and the newest values of α, σ, l and A immediately in succeeding calculations.

4. Another gravity solution is computed, using the data from the previous iteration as input data.

5. Step 4 is repeated until the results of two successive iterations differ by less than some specified amount, at which point computations are terminated. The solution to the gravity problem has then been found.

The method just described has several desirable features. It is direct and simple. It will theoretically produce a solution to any desired accuracy; one need only complete more iterative cycles to obtain a better solution. Practically, however, an iterative method of solution is useful in proportion to the rapidity of its convergence to the true solution. In this last regard the present method excels, having stabilized after only two complete iterative cycles in some typical cases to answers accurate to three significant figures.

The only drawback to this method is that the computation of one iteration is a lengthy process, even for a high-speed digital computer. The involved nature of the expressions being handled is the cause; specifically, the construction, by the use of a finite number of points and interpolation, of a reasonably accurate approximation to the continuous functions $J(t)$ and $J_l(t)$ is laborious. In fact, the work involved in obtaining a solution to the gravity problem is such that the use of a high-speed digital computer is mandatory. Methods of adapting the equations of §§3 and 4 so that they are more amenable to digital computations are given in Larock & Street (1966).

6. Discussion

Figure 5 indicates how the cavity streamlines and the various other parameters of the problem change when we iterate upon the initial non-gravity solution to obtain the solution to the gravity-affected problem. We note that k and t_B are held constant, and F^2 is prescribed. All the other parameters and results of the problem change; the direction of these changes can be noted from the figure.

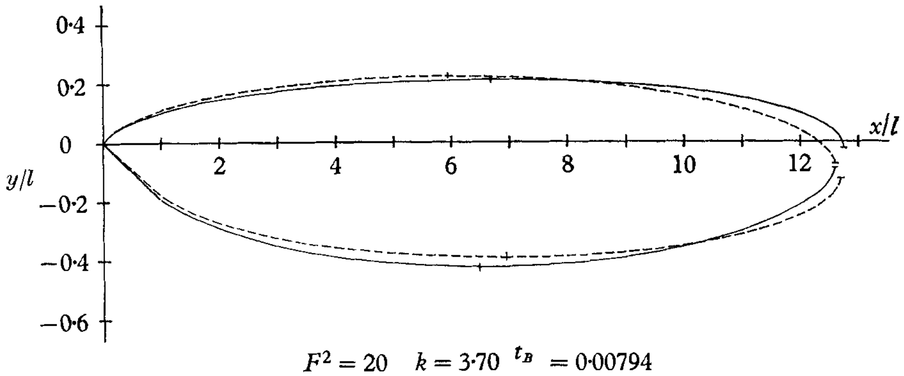

FIGURE 5. Cavity streamlines before and after iterations: the transverse gravity field effect. ---, before iteration, $\alpha = 10{\cdot}1^{\circ}$, $\sigma = 0{\cdot}100$, $C_L = 0{\cdot}249$, $C_D = 0{\cdot}0444$, $A = -0{\cdot}00640$, $l = 1{\cdot}165$; —, after iteration, $\alpha = 10{\cdot}7^{\circ}$, $\sigma = 0{\cdot}092$, $C_L = 0{\cdot}248$, $C_D = 0{\cdot}0469$, $A = -0{\cdot}00632$, $l = 1{\cdot}158$.

These quantities always vary in this fashion as a result of the iteration process. Knowledge of this behaviour is an aid in choosing the proper k and t_B for the problem of interest. In particular, α always increases and σ always decreases during the progression from initial approximation to final gravity solution. No quantitative rules have been established regarding these changes; however, a smaller value of F^2 produces larger relative changes in α and σ, and larger changes in α and σ occur when α and σ themselves are larger. Consequently, if we wish to choose k and t_B to produce a given α and σ in the presence of a gravity field, we choose the k and t_B which would produce a lower α and a higher σ than actually desired (see figure 4, Larock & Street 1965). This rule enables us to produce a gravity solution which is close to the one desired; thereafter, numerical experimentation is used to produce the precise α and σ desired. Thus, a gravity solution for a problem which is close to the desired solution is quickly found, but the solution for a precisely specified α and σ is more difficult and tedious to find.

A gravity solution for a given α and σ could be found by varying k and t_B in some fashion from iteration to iteration; we discard this approach for several reasons. Once k and t_B are set, the approximate size of all quantities in the solution has been set, since k and t_B are the two fundamental non-physical parameters of the basic equations. To vary k and t_B would then change all quantities in the problem in some relatively unpredictable fashion. Because the fundamental equations are non-linear, it would be very difficult to establish even qualitative rules for the systematic adjustment of k and t_B to achieve a given solution.

Section 5 indicated that the convergence of iterations to a stable solution is quite rapid. Table 1 shows this convergence for the case depicted in figure 5. Iteration 0 is the non-gravity solution. Essentially, the streamlines did not change position after the first iteration (figure 5). We see that the streamlines did shift position, however; the primary change is a slight rise in the streamlines toward the aft end of the cavity.

Iteration	α^0	σ	C_L
0	10·0928	0·100203	0·249392
1	10·6558	0·093689	0·249233
2	10·6950	0·092677	0·248544
3	10·6928	0·092540	0·248495

TABLE 1. Iterations of gravity solution

The effect of a transverse gravity field is seen most easily when we compare the gravity and non-gravity cases for the same attack angle and cavitation number. Two comparisons are presented in figures 6 and 7. In each case the gravity solution was constructed first, and a non-gravity solution was then matched to the gravity solution so that α and σ were the same.

Figure 6 matches the gravity solution of figure 5 with the equivalent non-gravity solution for $\alpha = 10{\cdot}7^\circ$ and $\sigma = 0{\cdot}092$. The non-gravity solution requires larger values of k and t_B than does the gravity solution. Also, the lift coefficient for the gravity solution is about 4 % lower than that for the non-gravity solution. The cavity for the gravity solution is significantly smaller than, and lies entirely within, the gravity-free cavity.

The real power of the present theory is graphically demonstrated in figure 7, which shows the gravity and non-gravity solutions for $\alpha = 32{\cdot}16^\circ$ and $\sigma = 0{\cdot}282$. By contrast, Parkin's (1957) linearized theory is limited to attack angles of 5° or less. For $\alpha = 32^\circ$, there is only a 2 % change in the lift coefficient due to the influence of the transverse gravity field, but there is a large difference in cavity size and shape.

The relation between cavitation number and lift coefficient for several Froude numbers at attack angles of 5° and 10° is depicted in figure 8. We note several items of interest. The effect of gravity is always to reduce the lift coefficient from that value which a gravity-free analysis predicts. For attack angles of 10° or less the effect of gravity on lift is always small and in many cases can be safely neglected. Moreover, the effect of gravity increases with decreasing cavitation number. This means that longer cavities are more greatly affected by gravity than are the shorter ones. As the attack angle increases, the effects of gravity persist to higher cavitation numbers, e.g. see figure 7 where $\sigma = 0{\cdot}282$. The lines corresponding to $F^2 = \infty$ were derived from the non-gravity solution of Larock & Street (1965).

The present theory is compared with Parkin's (1957) linearized transverse-gravity hydrofoil theory in figure 9. Parkin's problem is fully linearized with respect to both the boundary conditions and their points of application; the effect of gravity is approximated by the use of a constant, average-value gravity term on the cavity boundary. His non-gravity solution is obtained by setting the

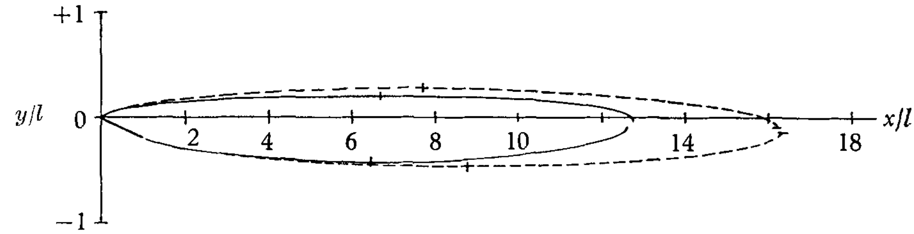

FIGURE 6. Effect of transverse gravity field, $\alpha = 10{\cdot}7^\circ$, $\sigma = 0{\cdot}092$, $F^2 = 20$. ----, no gravity, $k = 4{\cdot}25$, $t_B = 0{\cdot}0089$, $A = -0{\cdot}00515$, $C_L = 0{\cdot}259$, $C_D = 0{\cdot}0490$, $l = 1{\cdot}174$; —, gravity, $k = 3{\cdot}70$, $t_B = 0{\cdot}00794$, $A = -0{\cdot}00632$, $C_L = 0{\cdot}248$, $C_D = 0{\cdot}0469$, $l = 1{\cdot}158$.

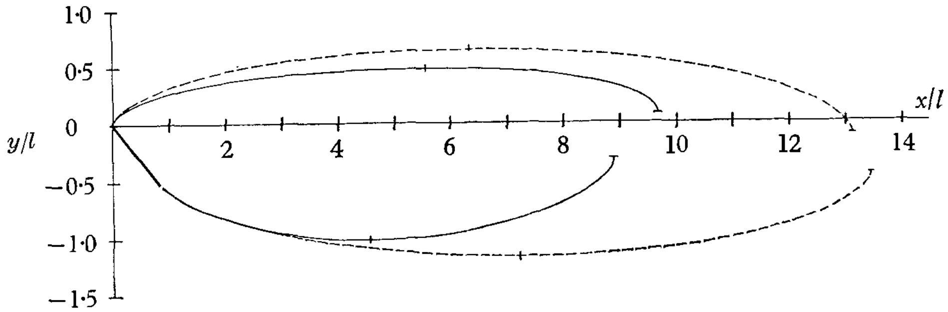

FIGURE 7. Effect of transverse gravity field, $\alpha = 32{\cdot}16^\circ$, $\sigma = 0{\cdot}282$, $F^2 = 9$. ----, no gravity, $k = 4{\cdot}656$, $t_B = 0{\cdot}08417$, $A = -0{\cdot}01326$, $C_L = 0{\cdot}510$, $C_D = 0{\cdot}321$, $l = 1{\cdot}695$; —, gravity, $k = 3{\cdot}750$, $t_B = 0{\cdot}07000$, $A = -0{\cdot}01783$, $C_L = 0{\cdot}504$, $C_D = 0{\cdot}317$, $l = 1{\cdot}581$.

average-value term to zero, and for $\alpha = 5^\circ$ his result is plotted on the figure. Also shown are Parkin's results for $F^2 = 16$ and the corresponding results from the present theory, all for $\alpha = 5^\circ$. Both with and without gravity, Parkin's theory gives higher values for the lift coefficient than does the present theory. This is consistent with his linearization method. In addition, Parkin's gravity effect is greater and persists to higher cavitation numbers than does that of the present theory. On the other hand, the theories agree generally and predict the same trends of behaviour.

The present theory and Parkin's theory agree on items other than lift-coefficient behaviour. Both theories predict that the gravity-affected cavity lies entirely within the non-gravity cavity. This agreement suggests that the result is a general one. Parkin also notes that longer cavities (low σ) are more affected by gravity than are the shorter ones (that this should be so is intuitively clear). This shortening of the cavity due to gravity effects has practical importance for designers who wish to estimate cavity length and shape as a factor in determining the possibilities of tandem foil interference and in establishing the thickness of the foil. These results could also have practical applications in future laboratory experiments.

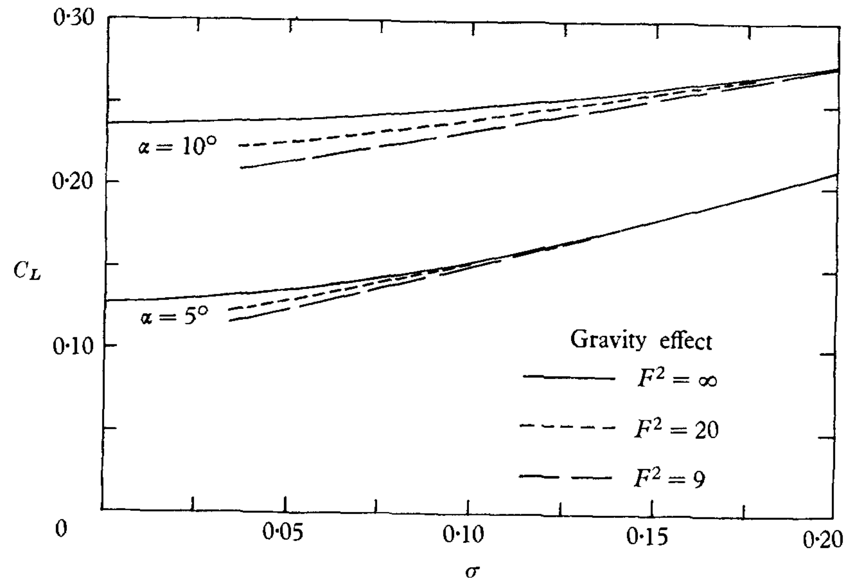

FIGURE 8. Effect of transverse gravity field on relation between lift coefficient and cavitation number.

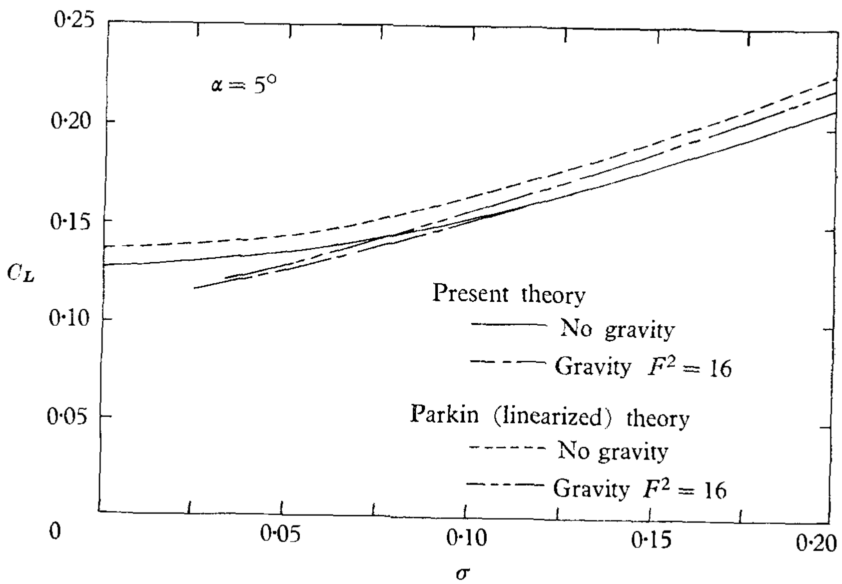

FIGURE 9. Lift coefficient *vs.* cavitation number: a comparison of linear and non-linear theory for $\alpha = 5°$ and $F^2 = 16$.

Finally, we would like to consider the case $\sigma = 0$ in the presence of gravity. In this case, however, it is not possible to approach the problem directly. We are thwarted because when $g = 0$ there is no close approximation to a finite cavity for $\sigma = 0$, although Tulin (1964*b*) indicates that a cavity of finite extent does exist for $\sigma = 0$ in the presence of gravity. There is an approach which appears fruitful, but it has not been tried because a sizeable amount of computer time seems to be needed and is not presently available. The approach is based on one of our earlier observations. When we iterate on a non-gravity solution where $\sigma > 0$, the attack angle increases and the cavitation number decreases under the influence of gravity. If an initial non-gravity solution is chosen which has a low cavitation number, it appears, for some particular Froude number, that the iteration process might very well produce a case where $\sigma = 0, g \neq 0$, and a finite cavity exists. This case appears worthy of future investigation.

The present results indicate that the effect of a transverse gravity field can be neglected in many practical cases. Indeed, if a 10 % error in force coefficients can be tolerated, then figure 8 shows that the influence of gravity can always be neglected for $\alpha \leqslant 10°$ and $\sigma \geqslant 0{\cdot}03$. We have also seen that lower Froude numbers indicate that larger gravity effects can be expected. (We might note here that for a hydrofoil craft with hydrofoils of 4 ft. chord, travelling at 35 knots = 50 ft./s, $F^2 = 27$.) However, because the cavity length and shape are important in many design considerations the effect of a gravity field always should be given consideration.

This research was carried out under the Bureau of Ships General Hydromechanics Research Programme, S-R009 01 01, administered by the David Taylor Model Basin, Office of Naval Research Contract Nonr 225(56). The major part of the computational work was supported by funds administered by the Stanford University Computation Centre. Reproduction in whole or in part is permitted for any purpose of the United States Government.

REFERENCES

ACOSTA, A. J. 1961 The effects of a longitudinal gravitational field on the supercavitating flow over a wedge. *J. Appl. Mech.*, **28**, *Trans. ASME*, **83** (Series E), 188–92.

CHENG, H. K. & ROTT, N. 1954 Generalizations of the inversion formula of thin airfoil theory. *J. Rat. Mech. Analysis*, **3**, 357–82.

CHURCHILL, R. V. 1960 *Complex Variables and Applications*, 2nd ed. New York: McGraw-Hill.

KICENIUK, T. & ACOSTA, A. J. 1966 Experiments on gravity effects in supercavitating flow. *J. Ship Res.* **10**, 119–21.

LAROCK, B. E. & STREET, R. L. 1965 A Riemann–Hilbert problem for nonlinear, fully cavitating flow. *J. Ship Res.* **9**, 170–8.

LAROCK, B. E. & STREET, R. L. 1966 A nonlinear theory for fully cavitating flows past an inclined flat plate. *Department of Civil Engng, Stanford University, Stanford, California*; *Tech. Rep.* no. 64.

LENAU, C. W. & STREET, R. L. 1965 A non-linear theory for symmetric, supercavitating flow in a gravity field. *J. Fluid Mech.* **21**, 257–80.

MIKHLIN, S. G. 1964 *Integral Equations* (translation by A. H. Armstrong). New York: Macmillan.

MILNE-THOMSON, L. M. 1960 *Theoretical Hydrodynamics*, 4th ed., p. 212. New York: Macmillan.

PARKIN, B. R. 1957 A note on the cavity flow past a hydrofoil in a liquid with gravity. *Engineering Division, California Institute of Technology, Pasadena, Rep.* no. 47–9.

PARKIN, B. R. 1959 Linearized theory of cavity flow in two dimensions. *RAND Corporation, Santa Monica, California, Rep.* no. P 1745.

SONG, C. S. 1963 A quasi-linear and linear theory for non-separated and separated two-dimensional, incompressible, irrotational flow about lifting bodies. *University of Minnesota, Minneapolis. SAF Hydraulic Lab. Tech. Paper*, no. 43 (Series B).

STREET, R. L. 1963 Supercavitating flow about a slender wedge in a transverse gravity field. *J. Ship Res.* **7**, 1, 14–23.

STREET, R. L. 1965 A note on gravity effects in supercavitating flow. *J. Ship Res.* **8**, 39–45.

TULIN, M. P. 1964*a* Supercavitating flows—small perturbation theory. *J. Ship Res.* **7**, 3.

TULIN, M. P. 1964*b* The shape of cavities in supercavitating flows. *XI IUTAM Congress Paper, Munich, Germany.*

WEINBERGER, H. F. 1965 *A First Course in Partial Differential Equations.* New York: Blaisdell.